Modeling individual lodgepole pine mortality from mountain pine beetle outbreak in a spatially explicit framework

Michele Susan Buonanduci

A thesis
submitted in partial fulfillment of the
requirements for the degree of

Master of Science

University of Washington

2019

Committee:

Brian J. Harvey, Chair

Patrick C. Tobin

E. Ashley Steel

Program Authorized to Offer Degree:
Quantitative Ecology and Resource Management

University of Washington

Abstract

Modeling individual lodgepole pine mortality from mountain pine beetle outbreak in a spatially explicit framework

Michele Susan Buonanduci

Chair of the Supervisory Committee:
Assistant Professor Brian J. Harvey
School of Environmental and Forest Sciences

Outbreaks of native bark beetles (*Curculionidae: Scolytinae*) are key natural disturbances that shape the structure and function of conifer forests across the northern hemisphere. While drivers of bark beetle outbreaks have been studied extensively at spatial scales ranging from stands to continents, within-stand processes driving individual tree mortality in an outbreak are less well understood. Here we use a spatially explicit long-term monitoring dataset of lodgepole pine (*Pinus contorta* var. *latifolia*) forest impacted by a severe mountain pine beetle (*Dendroctonus ponderosae*) outbreak to explore interactions among fine-scale drivers of beetle-caused tree mortality. Using a hierarchical Bayesian spatial modeling approach, we evaluated whether and how within-stand neighborhood structure and topographic setting interact with tree size to mediate tree level susceptibility to mountain pine beetle outbreak in the Southern Rocky Mountains (USA). We found evidence that both tree growth rate preceding the outbreak and stand structure around the host tree mediated the effect of tree size. However, we did not find evidence that topographic position within a stand mediated the effect of tree size. Mortality probability increased with pre-outbreak growth rate for small to medium sized trees (∼10-25 centimeters diameter), but that same effect could not be detected for larger trees. Conversely, mortality probability increased with greater neighborhood density across tree sizes, with the most pronounced effects for medium to

large sized trees (∼15-30 centimeters diameter). Within-stand topographic variability was not an important predictor of mortality probability; among stands, however, the driest stand conditions experienced the greatest overall mortality. By explicitly considering how natural within-stand heterogeneity mediates individual tree level susceptibility to mountain pine beetle outbreak, our findings bridge an important gap in understanding multi-scale drivers of disturbance dynamics. Identifying factors influencing individual tree mortality in these systems informs our understanding of both the structural development of forest stands and reciprocal feedbacks between stand structure and outbreak dynamics.

TABLE OF CONTENTS

LIST OF FIGURES

LIST OF TABLES

ACKNOWLEDGMENTS

First, I would like to thank my advisor, Brian Harvey. I am extraordinarily grateful for your mentorship and the opportunities you have provided. Thank you for taking a chance on me and for encouraging me every step of the way. To my committee members, Patrick Tobin and Ashley Steel: thank you for your insights and feedback. You have kept me honest and made this research stronger.

Thank you to the members of the Harvey Lab. Michelle Agne, Saba Saberi, and Jenna Morris: you have all had such a positive impact on my life. I couldn't have done this without you, for obvious reasons. Thank you to everyone in QERM, and in particular the 2017 cohort. Anne Polyakov and Colin Okasaki: you have both taught me so much. I couldn't have asked for two better people to start this journey with than you. Thank you to everyone in SEFS for welcoming me into your community. I feel so fortunate to have met, befriended, and learned so much from so many of you.

Finally, this project would not have been possible without the Fraser field crew. Felicity Carroll, Nicole Lau, Arielle Link, Aileen Liu, Sahale Riedel, and Thadeus Sternberg: thank you for your hard work and high spirits. Through wind, rain, lightning, and smoke, you carried on.

Chapter 1

INTERACTIVE EFFECTS OF TREE SIZE, GROWTH, AND NEIGHBORHOOD STRUCTURE ON MORTALITY FROM MOUNTAIN PINE BEETLE

1.1 Introduction

Native bark beetles (*Curculionidae: Scolytinae*) are one of the primary disturbance agents affecting temperate forests worldwide (Kautz et al., 2017; Sommerfeld et al., 2018). Through the selective mortality of host trees, bark beetle outbreaks substantially alter the size, age, and species distributions of forests within just a few years (Raffa et al., 2008). Outbreaks structure forests directly via mortality of overstory trees and indirectly by releasing the growth of understory trees as light, water, and nutrient availability all increase for survivors (Romme et al., 1986; Veblen et al., 1991). While bark beetle outbreaks are naturally occurring disturbance events in North American forests, recent outbreaks have been more intensive and spatially synchronous than previously recorded (Aukema et al., 2006; Bentz et al., 2009). Millions of hectares of forests in North America were impacted by bark beetle outbreaks in the period between 1997 and 2010, resulting in widespread tree mortality across multiple tree species (Meddens et al., 2012). Continued climate warming is projected to further alter outbreak dynamics (Bentz et al., 2010; Seidl et al., 2017), with significant implications for forest structure and function, in addition to the ecosystem services that forests provide (Raffa et al., 2008; Seidl et al., 2016; Thom and Seidl, 2016).

The mountain pine beetle (MPB; *Dendroctonus ponderosae*) is the most widespread biotic agent of tree mortality in western North American pine forests, affecting tens of millions of hectares of forest during episodic outbreaks (Safranyik and Carroll, 2006). MPB populations often persist at low, endemic levels, successfully attacking only weakened or damaged

Pinus trees. However, feedbacks among population controls (e.g., host availability and susceptibility, beetle density, weather, and climate) periodically enable populations to erupt into epidemic outbreaks (Raffa et al., 2008). At epidemic population densities, beetles are able to overcome vigorous host tree defenses through pheromone-mediated aggregation and mass attack (Boone et al., 2011; Raffa and Berryman, 1983; Safranyik and Carroll, 2006). Unconstrained by host tree defenses, epidemic populations will preferentially attack large diameter host trees with thicker phloem, which increase the reproductive and survival potential of the beetle (Safranyik and Carroll, 2006). Over the course of an outbreak, MPB are capable of killing 50% or more of host tree basal area within just a few years, as their colonization and reproduction essentially girdles the cambium and outer xylem of host trees (Diskin et al., 2011; Pelz and Smith, 2012; Simard et al., 2012). However, even in a severe outbreak (>80% of stand basal area killed), it is commonly observed that some of the largest host trees escape attack (e.g., Preisler and Mitchell, 1993), and the mechanisms responsible for this differential survival remain unresolved. Outbreak patterns and processes have been well studied at broad scales (e.g., continental to regional; Meddens et al., 2012) and at the among-stand level (i.e., aggregating all data to the stand; Simard et al., 2012). Dynamics at fine spatial scales (e.g., within a stand), which are important for understanding which trees are likely to survive an outbreak under particular conditions, are less well studied and understood.

Tree-level susceptibility to mortality in a beetle outbreak could result from interactions among several fine-scale factors that have not been empirically tested to date. Within-stand colonization patterns during MPB outbreak are driven strongly by host tree size; large diameter trees are preferentially attacked while small diameter trees are attacked primarily when in close proximity to large diameter trees (Kashian et al., 2011; Preisler and Mitchell, 1993). While these patterns appear to be consistent across stand densities and outbreak severities (Kashian et al., 2011; Preisler and Mitchell, 1993), it remains unclear how local (i.e., tree neighborhood level) stand structure and topography might mediate outbreak colonization patterns, and whether these effects vary with host tree size. Interactions among

factors at the tree scale and in the immediate environment of the tree are a key knowledge gap, with clear implications for understanding how MPB outbreaks alter stand structure and thus dynamics of future disturbances (Kashian et al., 2011). Integrating fine scale analyses into the broad-scale understanding of MPB outbreaks will build understanding of cross-scale drivers of disturbance dynamics. As the climate warms and broad scale constraints on outbreaks change (Bentz et al., 2010), fine-scale factors affecting outbreaks may be of increasing importance.

Here we used a spatially explicit long-term monitoring dataset of lodgepole pine (*Pinus contorta* var. *latifolia*) forest affected by a severe MPB outbreak (in Fraser Experimental Forest, FEF, Colorado) to characterize within-stand drivers of beetle-caused individual lodgepole pine mortality. We studied three 2-hectare (ha) plots in FEF in which every tree $\geq$5 cm in diameter (9,357 trees) was censused and measured leading up to and following a severe MPB outbreak to address the following research question: *How do tree level characteristics, neighborhood structure, and local topographic position interact to affect individual lodgepole pine mortality probability in a severe MPB outbreak?*

We expected that tree diameter would be the primary driver of mortality probability (Björklund and Lindgren, 2009), and that additional factors at the tree and tree neighborhood level would interact with tree size to mediate mortality probability. At the tree level, we expected that growth rates preceding the outbreak, a proxy for relative tree vigor, would have little or no effect on mortality probability given most tree defenses become ineffective once epidemic beetle population densities are reached (Boone et al., 2011). For this same reason, at the tree neighborhood level, we did not expect that reduced tree vigor from competition in dense neighborhoods would affect mortality probability in a severe outbreak. We did, however, expect mortality probability would be greater in high density neighborhoods due to more favorable microclimate for MPB (e.g., temperature and wind speed; Bartos and Amman, 1989) or preference of MPB for denser stands (Negrón, 2019). We also expected mortality would be greater in tree neighborhoods dominated by lodgepole pine due to high beetle pressure resulting from the emergence of adult MPB from neighboring colonized trees.

We expected that fine-scale topographic position would further mediate mortality probability since topoedaphic outbreak refugia (i.e., locations where impacts are less severe relative to the surrounding area) could exist at the stand scale (Cartwright, 2018). Finally, we expected that effects of pre-outbreak growth, neighborhood structure, and topographic position would differ by focal host tree size.

1.2 Methods

1.2.1 Study Area

FEF is located within the USA Southern Rockies Ecoregion, approximately 80 kilometers northwest of Denver, Colorado, in the Arapaho National Forest (Appendix A). The forests within FEF are composed primarily of lodgepole pine, subalpine fir (*Abies lasiocarpa*), and Engelmann spruce (*Picea engelmannii*). Lodgepole pine is the dominant tree species in lower elevational stands where the long-term monitoring plots are located, with subalpine fir and Engelmann spruce prevalent in the understory (Appendix A). The plots are located in >300 year old stands with no known stand-replacing disturbance since the stand-originating fire (Moir et al., Unpublished), with elevation ranging from 2,790 to 2,970 meters (m) (Appendix A, Appendix B). MPB activity was noted in FEF in 2003, had reached epidemic levels by 2006 (Hubbard et al., 2013), and had subsided by 2011 (Vorster et al., 2017). High rates of mortality of lodgepole pine were documented over the course of the outbreak, with MPB killing 90% of lodgepole pine trees over 30 centimeters (cm) in diameter (Rhoades et al., 2017).

1.2.2 Sampling Design

Three long-term monitoring plots (2 ha each) were established in 1938 (Wilm and Dunford, 1948), at which time a complete census was conducted of every living tree measuring at least 9 cm in diameter at breast height (DBH; measured 140 cm above the ground). The plots are separated by a minimum distance of 580 m and are each two ha in size (Appendix

A). Subsequent surveys were conducted in 1940, 1946, 1960, 1989, and 2004. DBH, tree morphology, and tree condition were recorded for each living tree, and mortality cause was determined for all dead trees that were living at the time of the previous survey. In 2004, the minimum diameter threshold for measurement was lowered to 5 cm and the tree population dataset was correspondingly expanded.

We conducted the first post-outbreak re-census of the plots in July and August 2018 and mapped the location of all live and dead surveyed trees (n = 9,357). Stem-mapping was conducted using FieldMap (Hédl et al., 2009; www.fieldmap.cz), a mobile stem-mapping unit that combines a laser rangefinder (TruPulse 360, Laser technology, Inc., USA) with geographic information system software. Standing trees were mapped in place, and uprooted trees were mapped at their previous rooted positions. Each tree was mapped with sub-meter accuracy to its horizontal coordinates (x,y) as well as its local elevation (z) relative to other trees.

The MPB outbreak in FEF began just prior to 2006 and had subsided by 2011 (Hubbard et al., 2013; Vorster et al., 2017). The pre-outbreak survey conducted in 2004 provides a census of the potentially susceptible population of lodgepole pine (n = 5,011), as well as the stand structure within each plot at the start of the outbreak. The post-outbreak survey conducted in 2018 provides the individual tree level survival outcomes (killed by MPB, not killed by MPB) within each plot (Fig. 1.1). Dead trees were recorded as "killed by MPB" only if MPB adult and larval galleries on the vascular cambium could be positively identified, following established methods (Safranyik and Carroll, 2006).

1.2.3 Tree Level Covariates

Tree size at the start of the outbreak was quantified using DBH recorded in the 2004 survey. The DBH recorded in 2004 was assumed to be the DBH of the tree at the time of MPB attack (i.e., any change in diameter that may have occurred over the course of the outbreak was considered negligible in this analysis). Growth rate preceding the outbreak was quantified as mean annualized basal area increment (BAI) estimated from DBH measurements recorded

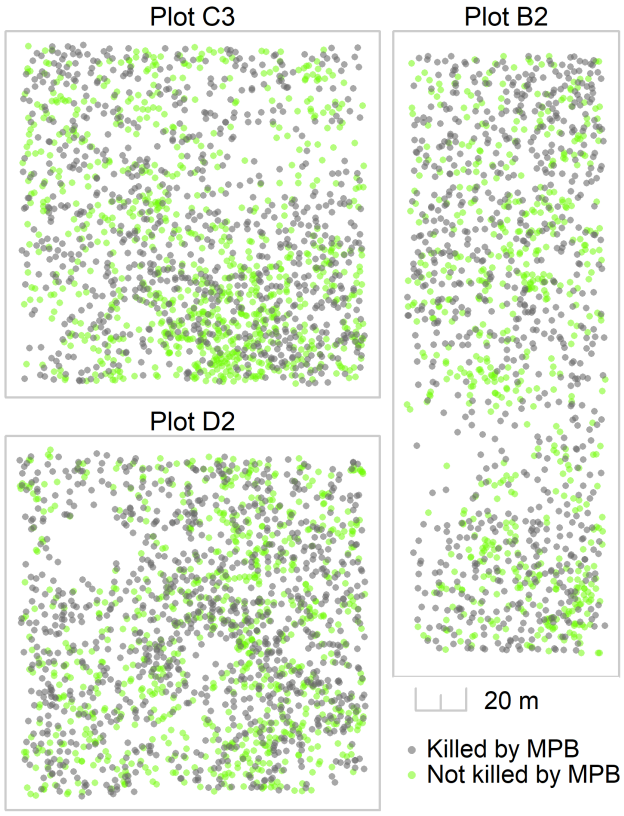

Figure 1.1: Stem maps illustrating post-outbreak mortality for all lodgepole pine ≥5 cm in diameter prior to the outbreak (gray = killed by MPB; green = not killed by MPB).

in 1989 and 2004. While tree growth is generally expected to follow a sigmoidal curve both with increasing age and with increasing size, using BAI rather than radial growth rates minimizes the effect of increasing circumference (Sullivan et al., 2016; Weiner and Thomas, 2001). We found a moderate positive correlation between DBH and BAI (Pearson r=0.5) in our dataset. However, variance inflation factors for all covariates included our analysis were <2, suggesting multicollinearity was of minimal concern. BAI estimates are below zero in some cases (7% of trees; Table 1.1), which we attribute to measurement error from slight differences in positioning of diameter tapes across surveys.

Metric	Statistic	Plot B2	Plot C3	Plot D2
Number of	Total	799	1,111	1,231
lodgepole pine	Killed by MPB	581	650	838
Diameter at breast	Min - Max	9.3 - 52.1	9.0 - 51.4	8.9 - 50.5
height	Mean	26.9	23.0	21.4
(DBH; cm)	Median	27.2	21.8	20.8
Basal area	Min - Max	-3.32 - 15.13	-2.50 - 16.80	-6.49 - 14.20
increment	Mean	2.36	2.17	1.86
(BAI; cm^2/year)	Median	1.95	1.67	1.48
Neighborhood	Min - Max	0.35 - 2.21	0.43 - 2.70	0.30 - 3.01
density index	Mean	1.11	1.30	1.23
(NDI; radians)	Median	1.09	1.24	1.19
Neighborhood host	Min - Max	0.00 - 1.00	0.13 - 1.00	0.16 - 1.00
proportion	Mean	0.90	0.92	0.97
(pNDI; unitless)	Median	0.94	0.97	1.00
Topographic	Min - Max	-1.51 - 0.72	-0.65 - 0.77	-0.78 - 1.13
position index	Mean	0.05	0.009	0.05
(TPI; m)	Median	0.06	0.005	0.04

Table 1.1: Descriptive statistics for dataset used in modeling. Dataset includes all lodgepole pine $\geq$5 cm in diameter at breast height that were alive in 2004 (pre-outbreak) and re-surveyed in 2018 (post-outbreak). Trees without pre-outbreak growth data (i.e., trees that were not surveyed in 1989) and trees <10 m from the edge of each plot were excluded from the dataset (n=3,141).

1.2.4 Neighborhood Level Covariates

Within-stand neighborhood density was quantified using the sum of horizontal angles originating from each focal tree center and spanning the DBH of each neighbor tree. This neighborhood density index (NDI) is calculated within a predetermined neighborhood radius as follows:

$$NDI = \sum_{i=1}^{n} arctan\left(\frac{DBH_i}{dist_i}\right),$$

where neighboring trees are indexed $i = 1, \ldots, n$; DBH_i is the diameter of neighboring tree i and $dist_i$ is the distance between the center of the focal tree and the center of neighboring tree i (Appendix C). NDI increases with increasing large, numerous, and/or close proximity trees in the neighborhood of the focal tree. While NDI was originally proposed as a tree competition index to characterize tree vigor (Rouvinen and Kuuluvainen, 1997), it also effectively serves as an index of relative stand density at the position inhabited by each tree. NDI was calculated using all neighboring trees, regardless of species. To quantify the relative density of host trees, we also calculated the proportion of total NDI contributed by lodgepole pine (pNDI).

Local topographic position was quantified using a topographic position index (TPI) that compares the elevation of each cell in a digital elevation model to the mean elevation of a specified neighborhood around that cell (Weiss, 2001). TPI is calculated as follows:

$$TPI = z_0 - \bar{z},$$

where z_0 is the elevation of the cell containing the focal tree and $\bar{z}$ is the average elevation around the focal tree within a predetermined radius. TPI is positive (convex local topography) when the focal tree is rooted in a position higher than its neighbors and negative (concave local topography) when the focal tree is rooted in a position lower than its neighbors (Appendix B). We calculated TPI using a digital elevation model constructed from the local elevation of each individual tree measured in the field.

Calculating neighborhood level covariates requires specifying the radius of the circular neighborhood that is considered. Ideally, the spatial scale of this neighborhood should be

informed by the ecological system. When characterizing tree competition effects, defining tree neighborhoods using a radius approximately 3.5 times the average estimated radius of tree crowns is appropriate (Contreras et al., 2011). We estimated that 10 m would be an appropriate neighborhood radius to consider, as mature lodgepole pine crowns range from 5 to 8 m in diameter (Herman et al., 1996). To avoid boundary effects, trees located <10 m from the edge of each plot were excluded from analysis. To test the sensitivity of neighborhood size, 5 m and 15 m neighborhoods were also considered and model results were compared.

1.2.5 Statistical Analysis

To make inference regarding the covariates potentially influencing MPB-induced mortality of lodgepole pine, we specified the following hierarchical generalized linear mixed effects model. The binary response (1 = killed by MPB, 0 = not killed by MPB) for lodgepole pine tree i, $i = 1 \dots n$ was modeled as a Bernoulli random variable Y_i measured at location s_i. The model takes the following form:

$$Y_i | p_i \sim Bernoulli(p_i)$$

$$log\left(\frac{p_i}{1-p_i}\right) = \beta_0 + \sum_{k=1}^{K} \beta_k x_{ik} + u_i,$$

where x_{ik} are K covariates and u_i is a continuous spatial Gaussian random field (GRF) measured at location s_i,

$$u_i(s_i) \sim GRF(0, \Sigma).$$

We defined the covariance matrix Σ using a Matérn covariance function parameterized by marginal standard deviation σ_u and practical range r (the distance at which the correlation drops to approximately 0.1; Krainski et al. 2019). We included tree level covariates (DBH, BAI; Table 1.1), neighborhood level covariates (NDI, pNDI, TPI; Table 1.1), and plot (B2, C3, D2) as fixed effects in the model. Because we expected that effects might vary with tree size, we also included interactions between DBH and all other tree and neighborhood level

covariates. To enable comparison of the magnitude of model coefficients, we standardized all covariates by subtracting their means and dividing by two times their standard deviations (Gelman, 2008).

We used the Integrated Nested Laplace Approximation (INLA) approach to implement this spatial model in a Bayesian framework. INLA is a deterministic algorithm developed to approximate posterior marginal distributions of model parameters (Rue et al., 2009) that offers substantial computational advantages when fitting spatial models (Blangiardo and Cameletti, 2015). To estimate the GRF at irregularly spaced point locations, we used the Stochastic Partial Differential Equation (SPDE) approach, which approximates the continuous GRF as a discrete Gaussian Markov random field (GMRF; Lindgren et al. 2011). The SPDE approach models the GMRF at the nodes of a triangulated grid (Appendix D) and then interpolates the GMRF throughout the study domain (Blangiardo and Cameletti, 2015; Lindgren et al., 2011).

Implementing the model in a Bayesian framework requires setting prior distributions for the model fixed effects and hyperparameters of the spatial random effect. We defined uninformative uniform and normal priors for the intercept and fixed effects, respectively. We set priors for the marginal standard deviation and practical range of the GRF using a Penalized Complexity prior (PC-prior) approach, which avoids spatial overfitting by shrinking the marginal variance toward zero (Fuglstad et al., 2019). The priors were defined as follows:

$$P(\sigma_u > 0.1) = 0.01$$

$$P(r < 30) = 0.5$$

The prior for the practical range r was set based on the a priori hypothesis that r might be close to 30 m, the typical dispersal distance of MPB in lodgepole pine forests (Safranyik and Carroll, 2006). Both the INLA and SPDE approaches were implemented in `R` (R Core Team, 2019) using the `R-INLA` package (www.r-inla.org).

We evaluated model fit via the conditional predictive ordinate (CPO; Pettit 1990), which is a *leave one out* cross-validation score. CPO is calculated for each observation Y_i by

omitting Y_i, fitting the model to all remaining observations $\mathbf{Y}_{-i}$, and then using the fitted model to predict the probability of Y_i. The sum of the log of the CPO values, also called the log pseudo marginal likelihood (LPML), is a useful summary of model fit, with larger sums indicating a better fitting model (Blangiardo and Cameletti, 2015). Since our primary goal was to evaluate whether within-stand spatial context mediates MPB-induced lodgepole pine mortality, we evaluated the fit of our model against the fit of (a) a model excluding neighborhood covariates, (b) a model excluding the random spatial effect, and (c) a model excluding both neighborhood covariates and the random spatial effect.

A covariate or interaction term x_k was considered an important predictor in the model if the 95% credible interval for the coefficient β_k did not include zero. To illustrate how both the size and position of a tree with a stand might affect its probability of mortality due to a severe MPB outbreak, we used the model to predict and produce maps of mortality probability across each plot for a range of tree sizes.

1.3 Results

Across all plots, 54% of lodgepole pine tree stems and 82% of lodgepole pine basal area were killed by MPB over the course of the outbreak. At the individual tree level, tree size was the most important factor driving MPB-induced lodgepole pine mortality; predicted mortality probability increased sharply for trees >15 cm diameter and the effect of DBH on mortality probability was approximately five times larger than other effects (Fig. 1.2, Fig. 1.3, Appendix E). The mean DBH of lodgepole pine killed by MPB was 27.1 cm (range 8.4 to 54.4 cm), and the mean DBH of lodgepole pine not killed by MPB was 13.0 cm (range 4.1 to 41.0 cm). While the main BAI term was not an important predictor of mortality probability, the DBH:BAI interaction term was negative, suggesting that the strength and direction of the effect of BAI depended on the focal tree size (Fig. 1.2, Appendix E). Greater BAI increased predicted mortality probability for small to medium diameter trees but had a negligible effect for large diameter trees (Fig. 1.3).

At the tree neighborhood level, the strength and direction of effects on mortality prob-

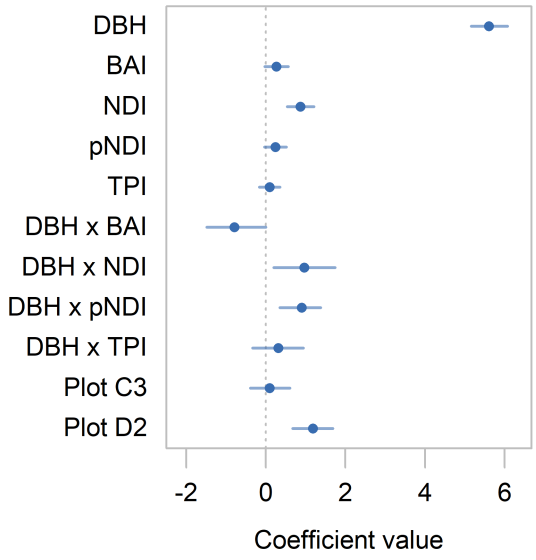

Figure 1.2: Effect of tree level covariates (DBH, BAI), tree neighborhood level covariates (NDI, pNDI, TPI), and plot on the probability of MPB-induced lodgepole pine mortality. Dots represent the medians of the posteriors and horizontal lines represent 95% credible intervals. A covariate or interaction term was considered an important predictor in the model if the 95% credible interval for the coefficient did not include zero. The effects for each continuous predictor are per 2 standard deviations in logit space.

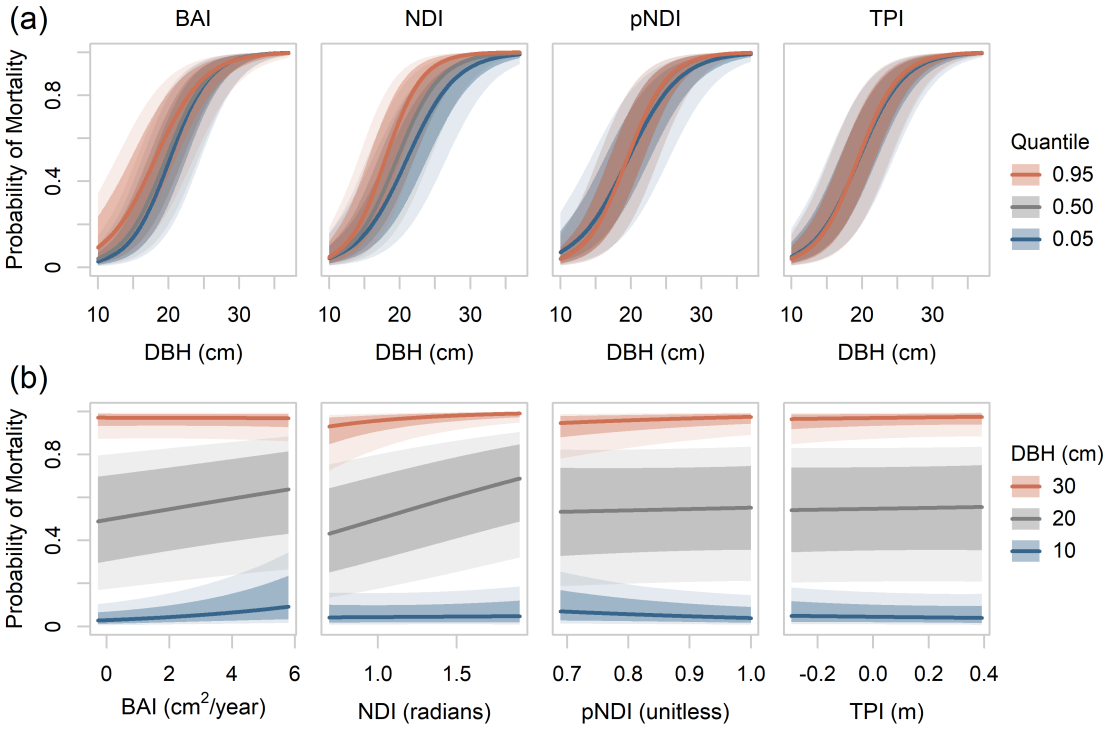

Figure 1.3: (a) Change in relationship between diameter at breast height (DBH; x-axis) and probability of mortality (y-axis) across gradients of basal area increment (BAI; column 1), neighborhood density index (NDI; column 2), neighborhood host proportion (pNDI; column 3), and topographic position index (TPI; column 4). (b) Change in relationship between covariates (x-axis) and probability of mortality (y-axis) across gradients of DBH. In both panels, solid lines represent posterior medians, and dark shaded regions represent 95% credible intervals modeled for one location within plot C3. Light shading represents variability in 95% credible intervals for locations across plot C3 (i.e., variability modeled by the spatial GRF). Predictions consider the effect of each combination of covariates in isolation, holding all other covariates at zero (i.e., their average values).

ability also depended on the size of the focal tree. A positive effect of NDI and a positive DBH:NDI interaction term (Fig. 1.2, Appendix E) suggest that neighborhood density contributes to MPB-induced lodgepole pine mortality, but effects vary by tree size. Greater NDI increased predicted mortality probability for medium to large diameter trees but had a negligible effect on mortality for small diameter trees (Fig. 1.3). While the main pNDI term was not an important predictor of mortality probability, the DBH:pNDI interaction term was positive (Fig. 1.2, Appendix E). Greater pNDI decreased predicted mortality probability for small-diameter trees and increased predicted mortality probability for large-diameter trees (Fig. 1.3). Neither TPI nor the DBH:TPI interaction term were important predictors (Fig. 1.2, Appendix E). At the plot level, plot D2 had a slightly higher mortality probability than plots B2 or C3 overall (Fig. 1.2, Appendix E).

The posterior median practical range of the spatial GRF was 31.7 m, with a posterior median marginal standard deviation of 0.51 (Appendix E). Spatial patterns of predicted mortality probability were comparable across the three plots, with the highest variability evident for trees of intermediate size (e.g., 15 to 25 cm DBH) and probabilities approaching zero and one for small and large diameter trees, respectively (Fig. 1.4). Accounting for effects of neighborhood level covariates and the spatial GRF resulted in substantially different predictions when compared to the model that considered only plot and tree level covariates, with differences in posterior median mortality probability estimates as large as ± 0.35 (Appendix F).

The model including neighborhood level covariates and the spatial GRF was the best fitting model that we evaluated. When building on a model that includes only plot and tree level covariates, adding neighborhood level covariates increased LPML by $\sim$19, adding the spatial GRF increased LPML by $\sim$46, and adding both neighborhood level covariates and the spatial GRF increased LPML by $\sim$63. Autocorrelation in the residuals of models without the spatial GRF indicated that including the spatial GRF was necessary to account for the spatial structure of the data. A sensitivity analysis of neighborhood size showed that the effect of changing the neighborhood radius by ± 5 m was negligible (Appendix G).

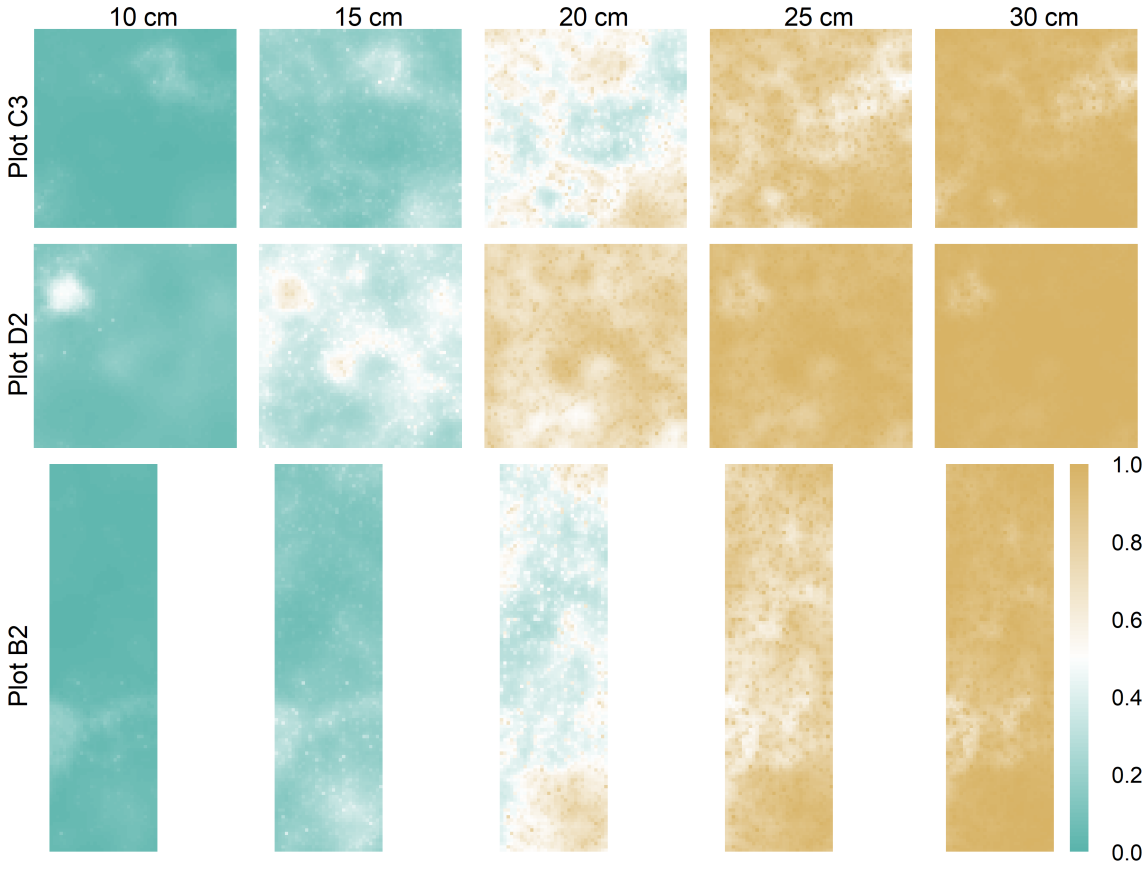

Figure 1.4: Spatial predictions of mortality probability for a range of lodgepole pine DBH (10 to 30 cm). Spatial predictions are posterior median predictions based on the specified DBH (columns) and the values of NDI, pNDI, and the spatial GRF for a hypothetical tree located within each grid cell in each plot (rows). BAI and TPI were held at zero (i.e., their average values).

1.4 Discussion

Explicitly considering how fine-scale patterns and processes can mediate the broad-scale drivers of disturbance dynamics is important as climate warms and disturbance activity increases. Our study demonstrates how natural within-stand heterogeneity can mediate individual tree level susceptibility to MPB outbreak, helping inform understanding of disturbance dynamics across scales. As expected, and consistent with previous research (Björklund and Lindgren, 2009; Kashian et al., 2011; Preisler and Mitchell, 1993), we found tree size to be the primary driver of lodgepole pine mortality probability in a severe MPB outbreak setting. Since MPB require a minimum phloem thickness to construct their galleries, small diameter host trees are often not capable of supporting MPB survival and reproduction, and large diameter host trees are preferred hosts (Safranyik and Carroll, 2006). Our model predictions suggest that for sufficiently small or sufficiently large diameter host trees, tree size largely overrides any within-stand mediating effects, with mortality probability approaching zero and one at 10 cm and 30 cm DBH, respectively. For host trees of intermediate size, however, we found that pre-outbreak growth rate and neighborhood stand structure (i.e., density and host proportion) may interact with tree size to mediate tree level susceptibility to severe MPB outbreak.

Our findings suggest that growth rate preceding an outbreak (measured here as BAI) may interact in key ways with tree size to affect mortality probability. We found that mortality probability increased with BAI for small to medium diameter trees (∼10-25 cm DBH), but the change in mortality probability with BAI appeared negligible for larger trees. Although contrary to our expectations, these results are consistent with recent research that found growth rates preceding an outbreak were positively related to mortality probability in lodgepole pine stands in Montana (Cooper et al., 2018). BAI may be a strong indicator of phloem thickness for lodgepole pine trees (Shrimpton and Thomson, 1985). It is possible that small diameter lodgepole pine, which otherwise may not be able to support MPB survival and reproduction, are more likely to be killed in an outbreak if they exhibit faster pre-outbreak

growth rates and thus potentially have thicker phloem. Conversely, fast growth rates did not negatively impact mortality probability for large diameter trees, as large trees already possess sufficient phloem thickness.

After accounting for tree size, we found that individual lodgepole pine mortality probability increased with neighborhood density, supporting our expectation. At the stand level, density may be positively related to MPB outbreak development, which has been explained with two potential mechanistic causes. Reduced competition in thinner stands can lead to increased vigor, and thus defensive capabilities, of host trees (e.g., Whitehead et al., 2005). In addition, sparse stands can have microclimate characteristics that are less favorable for MPB (e.g., higher temperature and wind speeds), resulting in a preference of MPB for denser stands (Bartos and Amman, 1989; Negrón, 2019). The increase in predicted mortality probability with NDI in our model suggests density at the neighborhood level may also mediate tree level mortality rates during MPB outbreak. Since host tree defenses become ineffective at epidemic beetle population levels (Boone et al., 2011), it is likely that the effect of neighborhood density is related to beetle preferences rather than tree defenses, particularly since tree vigor was more directly expressed by the BAI covariate in our model. While the interaction with tree diameter suggests that that the effect of neighborhood density is most pronounced for medium to large diameter lodgepole pine (∼15-30 cm DBH), being positioned in a lower density area may confer added tree-level resistance to MPB-induced mortality across tree sizes.

After accounting for neighborhood density, we found the proportion of neighborhood density contributed by lodgepole pine (i.e., pNDI) decreased predicted mortality probability for small diameter lodgepole pine (∼10-15 cm DBH) and increased predicted mortality probability for large diameter lodgepole pione (∼25-30 cm DBH). We expected to find a positive effect of pNDI due either to increased beetle pressure or increased intraspecific competition in areas dominated by lodgepole pine. The negative effect of pNDI for small diameter trees suggests the probability that small trees are killed by MPB is lower if they are rooted in an area dominated by other suitable host trees. This finding contradicts what has been found

in previous studies, which have reported that small host trees are more likely to be attacked by MPB when in close proximity to large host trees (e.g., Preisler and Mitchell, 1993). One possible explanation for our findings may be that increased intraspecific competition in areas dominated by lodgepole pine may lead to reduced growth rates and thus thinner phloem, as captured partially by the BAI covariate. However, the magnitude of the effect is modest when compared to the main effect of neighborhood density.

Our expectation that within-stand topographic position would affect tree level mortality probability was not supported in this study. While topographic effects may not be important at the within-stand spatial scales (e.g., sub meter) we analyzed, it is possible that local topographic position may mediate tree level mortality probability in more topographically complex stands or at broader spatial scales (e.g., several hectares). For example, at broader scales (among stands), outbreak refugia in topographically concave areas may be linked to cool, moist conditions, which potentially relieve tree stress during drought conditions and reduce likelihood of MPB infestation (Cartwright, 2018). Our data provide some support for this effect among stands, as the mortality rate was greatest in D2, the plot with the steepest slope and the most southwesterly aspect (Appendix A), characteristics that relate to faster runoff, less infiltration, warmer conditions, and drier soils (Cartwright, 2018).

The spatial GRF in our model accounts for deviations from the pattern of mortality and survival predicted using fixed effects at the tree, neighborhood, and plot level. These deviations may represent variation in the probability of mortality due to environmental factors or tree-level physiological factors (Zhao and Erbilgin, 2019) not considered in this study, or as variation in the probability of mortality due to the beetle-generated semiochemical landscape. Given the stochastic nature of beetle dynamics and the switching that occurs from focal to neighboring trees during outbreak (Preisler and Mitchell, 1993), there is inherent clustering in MPB outbreak dynamics. It is possible that the spatial GRF captures some of this inherent clustering.

The interactions among tree level and tree neighborhood level factors in this study have important implications for tree level resistance to MPB outbreak. Because the biology of

MPB places constraints on which trees may act as suitable hosts, and these constraints are linked tightly to tree size (Safranyik and Carroll, 2006), the strength and direction of potential mediating effects cannot be considered in the absence of tree size. We found that pre-outbreak growth rates and tree neighborhood structure had the greatest effect on predicted mortality probability for trees of intermediate size (e.g., 15 to 25 cm DBH; Fig. 1.3). Previous research has suggested that lodgepole pine trees <25 cm in diameter are beetle "sinks" (i.e., more beetles attack than emerge; Safranyik and Carroll, 2006). In this intermediate range, trees are large enough to physically support MPB survival and reproduction, yet not large enough that they would be considered the most desirable hosts. It is in these cases that mediating factors such as pre-outbreak growth rate, neighborhood stand density, and neighborhood host proportion may have a meaningful effect.

The tree level mortality probability modeled in this study is the probability that an individual lodgepole pine will be killed by MPB over the course of an outbreak, given that an outbreak has occurred. This probability differs from both (a) the probability that an individual lodgepole pine will be killed by MPB at endemic population levels, where different processes and dynamics would be expected at both the tree and neighborhood level; and (b) the probability of an outbreak developing within a stand, which is the focus of stand level hazard and risk ratings for MPB (Shore et al., 2000). In this study, we treat tree level and tree neighborhood level characteristics at the start of an outbreak as static factors influencing subsequent outbreak dynamics. However, we note that these factors (tree size, growth rates, and neighborhood structure) are not static in any stand. The timing of outbreaks is a critical component determining how MPB outbreak may affect a particular stand impacted at a particular time. We also acknowledge that temporal dynamics over the course of an outbreak and interactions with other biotic disturbances are important to consider. Incorporating these dynamics and interactions would be important contributions of future research.

While our results suggest that tree level mortality probability may be higher in denser portions of a stand during MPB outbreak, we emphasize that our study was conducted in plots without any prior management. While thinning stands has the potential to reduce the

probability of outbreak development (Fettig et al., 2007), it is unclear to what extent thinned stands confer resistance to MPB at the individual tree level in the event MPB outbreak does occur.

1.5 Conclusion

Conifer forests have been shaped by periodic bark beetle outbreaks for millennia (Jarvis and Kulakowski, 2015; Raffa et al., 2008). Understanding the causes and effects of bark beetle outbreaks across scales is particularly important as climate warms and environmental constraints change (Bentz et al., 2010). Our findings suggest that while tree size is the primary factor driving host tree mortality during MPB outbreak, pre-outbreak growth and neighborhood stand structure may mediate mortality probability in meaningful ways. Further, the direction and magnitude of these mediating effects may vary with tree size. The interactions among tree level and tree neighborhood level factors in this study highlight the importance of natural within-stand heterogeneity in conferring resistance to disturbance. Identifying factors influencing within-stand tree mortality enhances our understanding of outbreak dynamics, with implications for the structural development of forest stands and feedbacks among disturbances.

1.6 Acknowledgements

We thank the U.S. Forest Service Rocky Mountain Research Station, K. Elder, B. Starr, and D. McClain for facilitating access to field sites and housing in the Fraser Experimental Forest. We thank F. Carroll, N. Lau, A. Link, A. Liu, S. Riedel, and R. T. Sternberg for field assistance and data entry, and E. Vilanova for FieldMap training. This work would not have been possible without the 1989 and 2004 surveys led by J. Franklin, W. Moir, and M. Harmon; we are extraordinarily grateful for the meticulous data collection of their field crews and for the data curation of R. Pabst. We are grateful for insight provided by J. Negrón, M. Battaglia, and C. Rhoades, and for feedback provided by P. Tobin, E. A. Steel, T. Veblen, and R. Andrus. This work is supported by the McIntire-Stennis Cooperative Forestry Research

Program (grant no. NI17MSCFRXXXG003/project accession no. 1012773) from the USDA National Institute of Food and Agriculture. Additional funding was provided by the School of Environmental and Forest Sciences, the Quantitative Ecology and Resource Management Program, and the Student Technology Fee at the University of Washington.

REFERENCES

Aukema, B. H., Carroll, A. L., Zhu, J., Raffa, K. F., Sickley, T. A., and Taylor, S. W. (2006). Landscape level analysis of mountain pine beetle in british columbia, canada: spatiotemporal development and spatial synchrony within the present outbreak. *Ecography*, 29(3):427–441.

Bartos, D. L. and Amman, G. D. (1989). Microclimate: an alternative to tree vigor as a basis for mountain pine beetle infestations. *Res. Pap. INT-RP-400. Ogden, UT: US Department of Agriculture, Forest Service, Intermountain Research Station. 10 p.*, 400.

Bentz, B., Logan, J., MacMahon, J., Allen, C. D., Ayres, M., Berg, E., Carroll, A., Hansen, M., Hicke, J., Joyce, L., et al. (2009). Bark beetle outbreaks in western north america: Causes and consequences. In *Bark Beetle Symposium; Snowbird, Utah; November, 2005. Salt Lake City, UT: University of Utah Press. 42 p.*

Bentz, B. J., Régnière, J., Fettig, C. J., Hansen, E. M., Hayes, J. L., Hicke, J. A., Kelsey, R. G., Negrón, J. F., and Seybold, S. J. (2010). Climate change and bark beetles of the western united states and canada: direct and indirect effects. *BioScience*, 60(8):602–613.

Björklund, N. and Lindgren, B. S. (2009). Diameter of lodgepole pine and mortality caused by the mountain pine beetle: factors that influence their relationship and applicability for susceptibility rating. *Canadian journal of forest research*, 39(5):908–916.

Blangiardo, M. and Cameletti, M. (2015). *Spatial and spatio-temporal Bayesian models with R-INLA*. John Wiley & Sons.

Boone, C. K., Aukema, B. H., Bohlmann, J., Carroll, A. L., and Raffa, K. F. (2011). Efficacy

of tree defense physiology varies with bark beetle population density: a basis for positive feedback in eruptive species. *Canadian Journal of Forest Research*, 41(6):1174–1188.

Cartwright, J. (2018). Landscape topoedaphic features create refugia from drought and insect disturbance in a lodgepole and whitebark pine forest. *Forests*, 9(11):715.

Contreras, M. A., Affleck, D., and Chung, W. (2011). Evaluating tree competition indices as predictors of basal area increment in western montana forests. *Forest Ecology and Management*, 262(11):1939–1949.

Cooper, L. A., Reed, C. C., and Ballantyne, A. P. (2018). Mountain pine beetle attack faster growing lodgepole pine at low elevations in western montana, usa. *Forest ecology and management*, 427:200–207.

Diskin, M., Rocca, M. E., Nelson, K. N., Aoki, C. F., and Romme, W. (2011). Forest developmental trajectories in mountain pine beetle disturbed forests of rocky mountain national park, colorado. *Canadian Journal of Forest Research*, 41(4):782–792.

Fettig, C. J., Klepzig, K. D., Billings, R. F., Munson, A. S., Nebeker, T. E., Negrón, J. F., and Nowak, J. T. (2007). The effectiveness of vegetation management practices for prevention and control of bark beetle infestations in coniferous forests of the western and southern united states. *Forest ecology and management*, 238(1-3):24–53.

Fuglstad, G.-A., Simpson, D., Lindgren, F., and Rue, H. (2019). Constructing priors that penalize the complexity of gaussian random fields. *Journal of the American Statistical Association*, 114(525):445–452.

Gelman, A. (2008). Scaling regression inputs by dividing by two standard deviations. *Statistics in medicine*, 27(15):2865–2873.

Hédl, R., Svátek, M., Dančák, M., Rodzay, A., Salleh, A., Kamariah, A., et al. (2009). A new technique for inventory of permanent plots in tropical forests: a case study from lowland

dipterocarp forest in kuala belalong, brunei darussalam. *Blumea-Biodiversity, Evolution and Biogeography of Plants*, 54(1-2):124–130.

Herman, D. E., Stange, C. M., and Quam, V. C. (1996). *North Dakota tree handbook*. North Dakota State Soil Conservation Committee.

Hubbard, R. M., Rhoades, C. C., Elder, K., and Negron, J. (2013). Changes in transpiration and foliage growth in lodgepole pine trees following mountain pine beetle attack and mechanical girdling. *Forest Ecology and Management*, 289:312–317.

Jarvis, D. S. and Kulakowski, D. (2015). Long-term history and synchrony of mountain pine beetle outbreaks in lodgepole pine forests. *Journal of Biogeography*, 42(6):1029–1039.

Kashian, D. M., Jackson, R. M., and Lyons, H. D. (2011). Forest structure altered by mountain pine beetle outbreaks affects subsequent attack in a wyoming lodgepole pine forest, usa. *Canadian journal of forest research*, 41(12):2403–2412.

Kautz, M., Meddens, A. J., Hall, R. J., and Arneth, A. (2017). Biotic disturbances in northern hemisphere forests–a synthesis of recent data, uncertainties and implications for forest monitoring and modelling. *Global Ecology and Biogeography*, 26(5):533–552.

Krainski, E. T., Gómez-Rubio, V., Bakka, H., Lenzi, A., Castro-Camilo, D., Simpson, D., Lindgren, F., and Rue, H. (2019). *Advanced spatial modeling with stochastic partial differential equations using R and INLA*. Chapman and Hall/CRC.

Lindgren, F., Rue, H., and Lindström, J. (2011). An explicit link between gaussian fields and gaussian markov random fields: the stochastic partial differential equation approach. *Journal of the Royal Statistical Society: Series B (Statistical Methodology)*, 73(4):423–498.

Meddens, A. J., Hicke, J. A., and Ferguson, C. A. (2012). Spatiotemporal patterns of observed bark beetle-caused tree mortality in british columbia and the western united states. *Ecological Applications*, 22(7):1876–1891.

Moir, W., Harmon, M., Hawksworth, F., Brainerd, R., and Franklin, J. (Unpublished). Fifty years of succession in old-growth lodgepole pine and spruce-fir forests in colorado. Unpublished manuscript.

Negrón, J. (2019). Biological aspects of mountain pine beetle in lodgepole pine stands of different densities in colorado, usa. *Forests*, 10(1):18.

Pelz, K. A. and Smith, F. W. (2012). Thirty year change in lodgepole and lodgepole/mixed conifer forest structure following 1980s mountain pine beetle outbreak in western colorado, usa. *Forest Ecology and Management*, 280:93–102.

Pettit, L. (1990). The conditional predictive ordinate for the normal distribution. *Journal of the Royal Statistical Society: Series B (Methodological)*, 52(1):175–184.

Preisler, H. K. and Mitchell, R. G. (1993). Colonization patterns of the mountain pine beetle in thinned and unthinned lodgepole pine stands. *Forest Science*, 39(3):528–545.

R Core Team (2019). *R: A Language and Environment for Statistical Computing*. R Foundation for Statistical Computing, Vienna, Austria.

Raffa, K. and Berryman, A. (1983). The role of host plant resistance in the colonization behavior and ecology of bark beetles (coleoptera: Scolytidae). *Ecological monographs*, 53(1):27–49.

Raffa, K. F., Aukema, B. H., Bentz, B. J., Carroll, A. L., Hicke, J. A., Turner, M. G., and Romme, W. H. (2008). Cross-scale drivers of natural disturbances prone to anthropogenic amplification: the dynamics of bark beetle eruptions. *Bioscience*, 58(6):501–517.

Rhoades, C. C., Hubbard, R. M., and Elder, K. (2017). A decade of streamwater nitrogen and forest dynamics after a mountain pine beetle outbreak at the fraser experimental forest, colorado. *Ecosystems*, 20(2):380–392.

Romme, W. H., Knight, D. H., and Yavitt, J. B. (1986). Mountain pine beetle outbreaks in the rocky mountains: regulators of primary productivity? *The American Naturalist*, 127(4):484–494.

Rouvinen, S. and Kuuluvainen, T. (1997). Structure and asymmetry of tree crowns in relation to local competition in a natural mature scots pine forest. *Canadian Journal of Forest Research*, 27(6):890–902.

Rue, H., Martino, S., and Chopin, N. (2009). Approximate bayesian inference for latent gaussian models by using integrated nested laplace approximations. *Journal of the royal statistical society: Series b (statistical methodology)*, 71(2):319–392.

Safranyik, L. and Carroll, A. L. (2006). The biology and epidemiology of the mountain pine beetle in lodgepole pine forests. In Safranyik, L. and Wilson, B., editors, *The Mountain Pine Beetle: A Synthesis of Its Biology, Management and Impacts on Lodgepole Pine*, pages 3–66. Canadian Forest Service, Pacific Forestry Centre, Natural Resources Canada, Victoria, Canada.

Seidl, R., Spies, T. A., Peterson, D. L., Stephens, S. L., and Hicke, J. A. (2016). Searching for resilience: addressing the impacts of changing disturbance regimes on forest ecosystem services. *Journal of applied ecology*, 53(1):120–129.

Seidl, R., Thom, D., Kautz, M., Martin-Benito, D., Peltoniemi, M., Vacchiano, G., Wild, J., Ascoli, D., Petr, M., Honkaniemi, J., et al. (2017). Forest disturbances under climate change. *Nature climate change*, 7(6):395.

Shore, T., Safranyik, L., and Lemieux, J. (2000). Susceptibility of lodgepole pine stands to the mountain pine beetle: testing of a rating system. *Canadian Journal of Forest Research*, 30(1):44–49.

Shrimpton, D. and Thomson, A. (1985). Relationship between phloem thickness and lodgepole pine growth characteristics. *Canadian Journal of Forest Research*, 15(5):1004–1008.

Simard, M., Powell, E. N., Raffa, K. F., and Turner, M. G. (2012). What explains landscape patterns of tree mortality caused by bark beetle outbreaks in greater yellowstone? *Global Ecology and Biogeography*, 21(5):556–567.

Sommerfeld, A., Senf, C., Buma, B., D'Amato, A. W., Després, T., Díaz-Hormazábal, I., Fraver, S., Frelich, L. E., Gutiérrez, Á. G., Hart, S. J., et al. (2018). Patterns and drivers of recent disturbances across the temperate forest biome. *Nature Communications*, 9(1):4355.

Sullivan, P. F., Pattison, R. R., Brownlee, A. H., Cahoon, S. M., and Hollingsworth, T. N. (2016). Effect of tree-ring detrending method on apparent growth trends of black and white spruce in interior alaska. *Environmental Research Letters*, 11(11):114007.

Thom, D. and Seidl, R. (2016). Natural disturbance impacts on ecosystem services and biodiversity in temperate and boreal forests. *Biological Reviews*, 91(3):760–781.

Veblen, T. T., Hadley, K. S., Reid, M. S., and Rebertus, A. J. (1991). The response of subalpine forests to spruce beetle outbreak in colorado. *Ecology*, 72(1):213–231.

Vorster, A. G., Evangelista, P. H., Stohlgren, T. J., Kumar, S., Rhoades, C. C., Hubbard, R. M., Cheng, A. S., and Elder, K. (2017). Severity of a mountain pine beetle outbreak across a range of stand conditions in fraser experimental forest, colorado, united states. *Forest ecology and management*, 389:116–126.

Weiner, J. and Thomas, S. C. (2001). The nature of tree growth and the "age-related decline in forest productivity". *Oikos*, 94(2):374–376.

Weiss, A. (2001). Topographic position and landforms analysis. In *Poster presentation, ESRI user conference, San Diego, CA*, volume 200.

Whitehead, R. J., Russo, G. L., et al. (2005). *Beetle-proofed lodgepole pine stands in interior British Columbia have less damage from mountain pine beetle*, volume 402. Pacific Forestry Centre.

Wilm, H. G. and Dunford, E. G. (1948). Effect of timber cutting on water available for stream flow from a lodgepole pine forest. Technical report, US Department of Agriculture.

Zhao, S. and Erbilgin, N. (2019). Larger resin ducts are linked to the survival of lodgepole pine trees during mountain pine beetle outbreak. *Frontiers in Plant Science*, 10:1459.

Appendix A

SITE DESCRIPTION

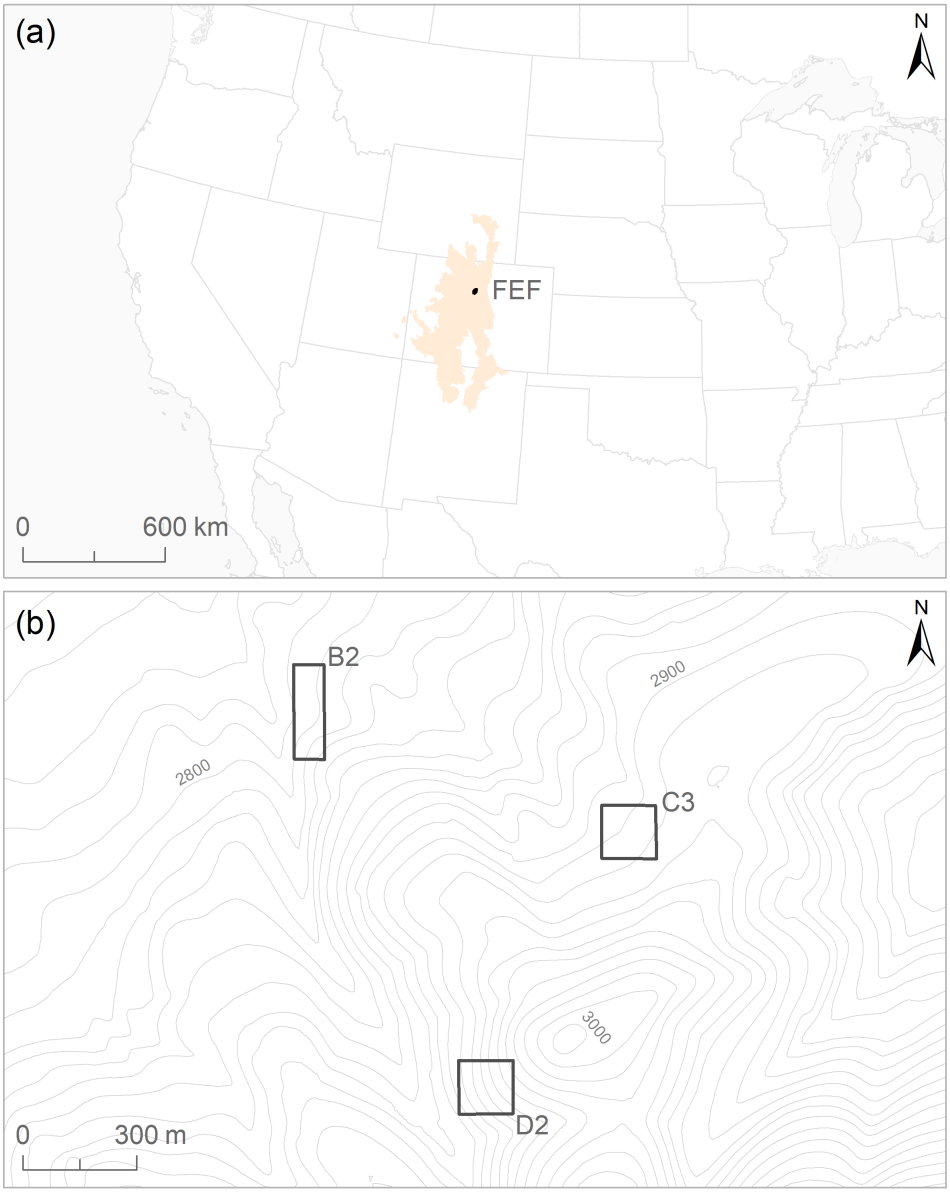

Figure A.1: (a) The Fraser Experimental Forest (FEF) is located within the Southern Rockies Ecoregion (orange shading) in Colorado, USA. (b) Long-term monitoring plots (black outline) are separated by a minimum distance of 580 meters and are each two hectares in size.

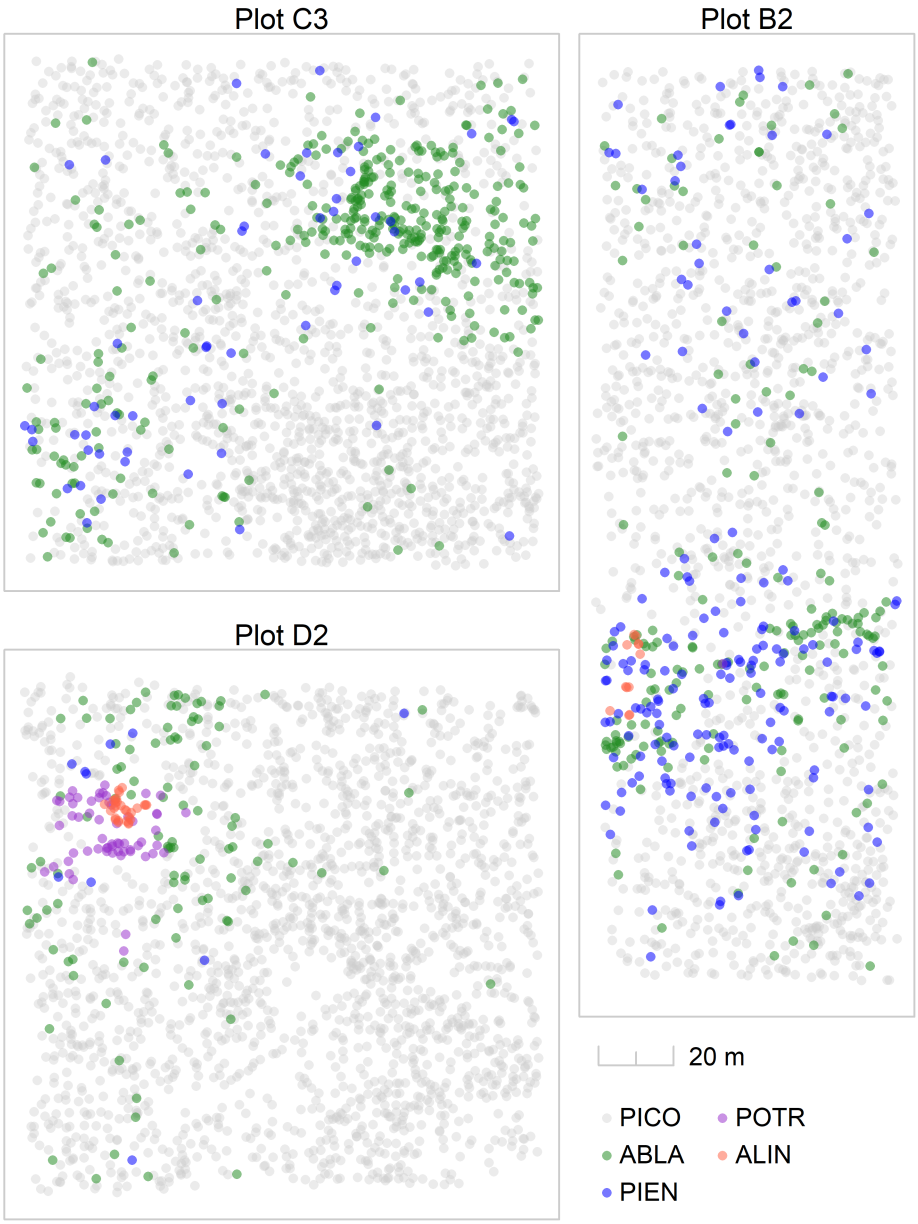

Figure A.2: Stem maps of pre-outbreak species composition (i.e., all live trees ≥5 cm DBH in 2004). Stem maps include lodgepole pine (*Pinus contorta* var. *latifolia*; PICO), subalpine fir (*Abies lasiocarpa*; ABLA), Engelmann spruce (*Picea engelmannii*; PIEN), quaking aspen (*Populus tremuloides*; POTR), and grey alder (*Alnus incana*; ALIN). Scouler's willow (*Salix scouleriana*) and Douglas fir (*Pseudotsuga menziesii*), which are present in the plots in negligible quantities, are excluded from the figure.

Plot	Species	Pre-outbreak (2004)		Post-outbreak (2018)	
		Stem density (stems/ha)	Basal area (m^2/ha)	Stem density (stems/ha)	Basal area (m^2/ha)
B2	*Abies lasiocarpa*	94.0	1.37	154.0	2.13
	Alnus incana	6.0	0.03	9.0	0.04
	Pinus contorta	706.0	34.43	456.0	6.03
	Picea engelmannii	90.5	4.01	116.5	4.51
	Populus tremuloides	0.5	0.01	0.5	0.01
	Total	897.0	39.85	736.0	12.72
C3	*Abies lasiocarpa*	188.5	2.33	303.5	4.05
	Pinus contorta	856.0	35.08	433.0	8.11
	Picea engelmannii	29.0	0.85	39.0	0.95
	Salix scouleriana	0.5	0.005	0.0	0.00
	Total	1074.0	38.26	775.5	13.10
D2	*Abies lasiocarpa*	50.0	0.81	71.5	1.54
	Alnus incana	14.5	0.08	22.0	0.11
	Pinus contorta	943.5	33.06	411.0	6.45
	Picea engelmannii	5.0	0.32	8.0	0.30
	Populus tremuloides	29.5	0.32	15.5	0.24
	Pseudotsuga menziesii	0.5	0.001	0.5	0.004
	Salix scouleriana	0.5	0.003	1.5	0.01
	Total	1043.5	34.60	530.0	8.66

Table A.1: Descriptive statistics of pre- and post-outbreak plot stand structure. Stem density and basal area calculated for all live trees $\geq$5 cm in diameter at breast height.

Appendix B

PLOT TOPOGRAPHY

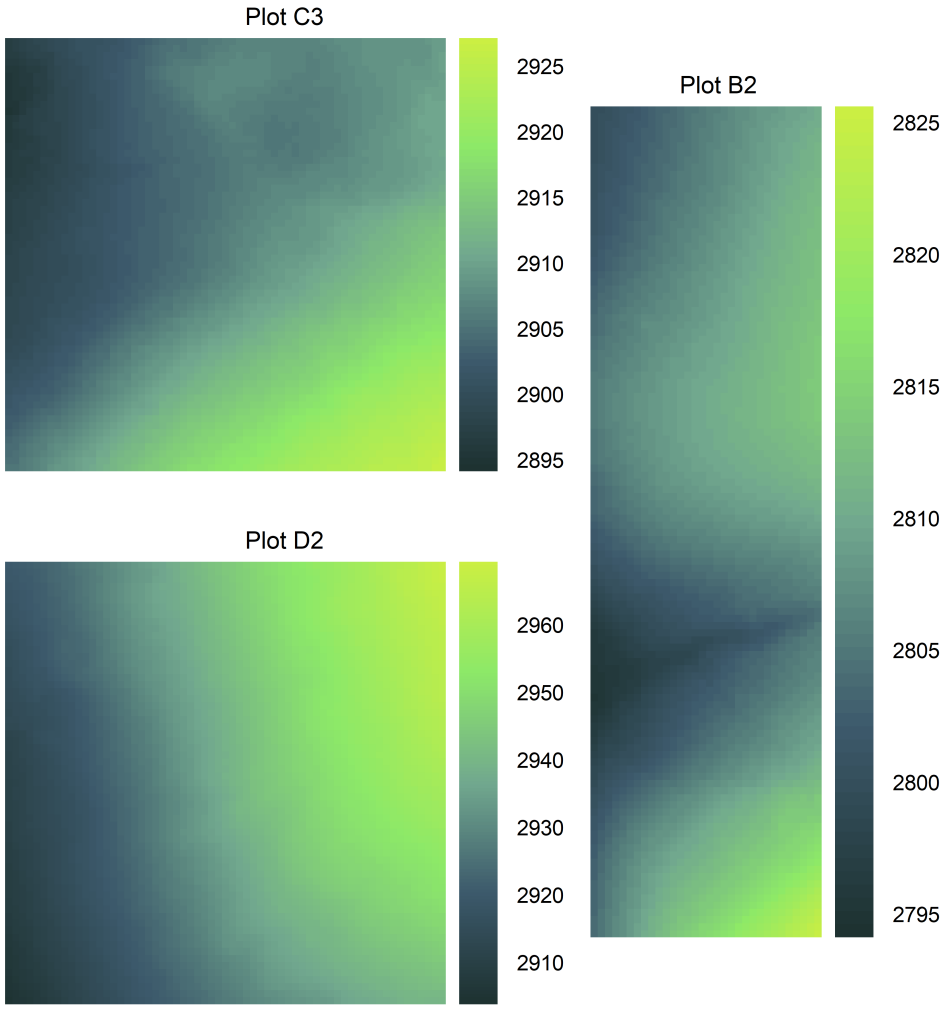

Figure B.1: Plot elevation (m).

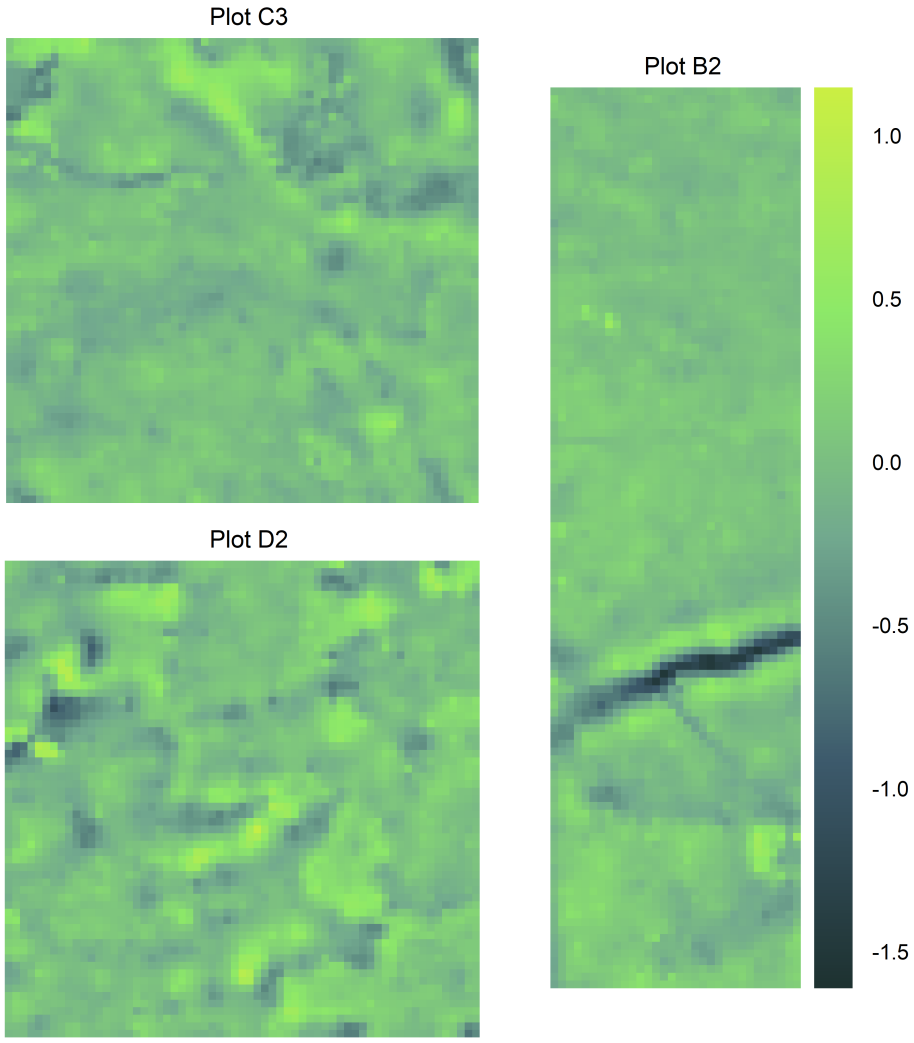

Figure B.2: Plot topographic position index (m).

Appendix C

PLOT STAND STRUCTURE

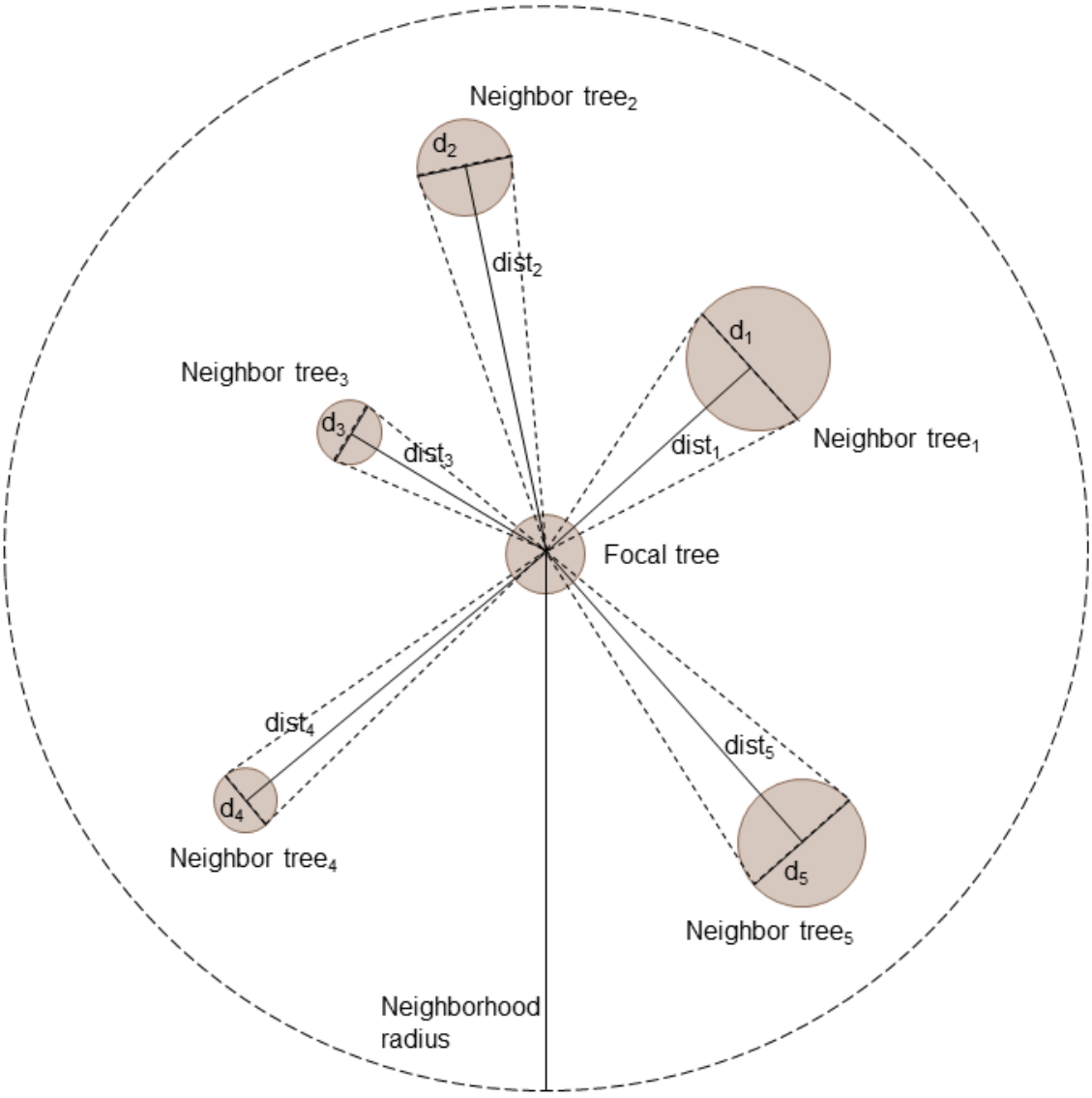

Figure C.1: Schematic illustrating calculation of the neighborhood density index

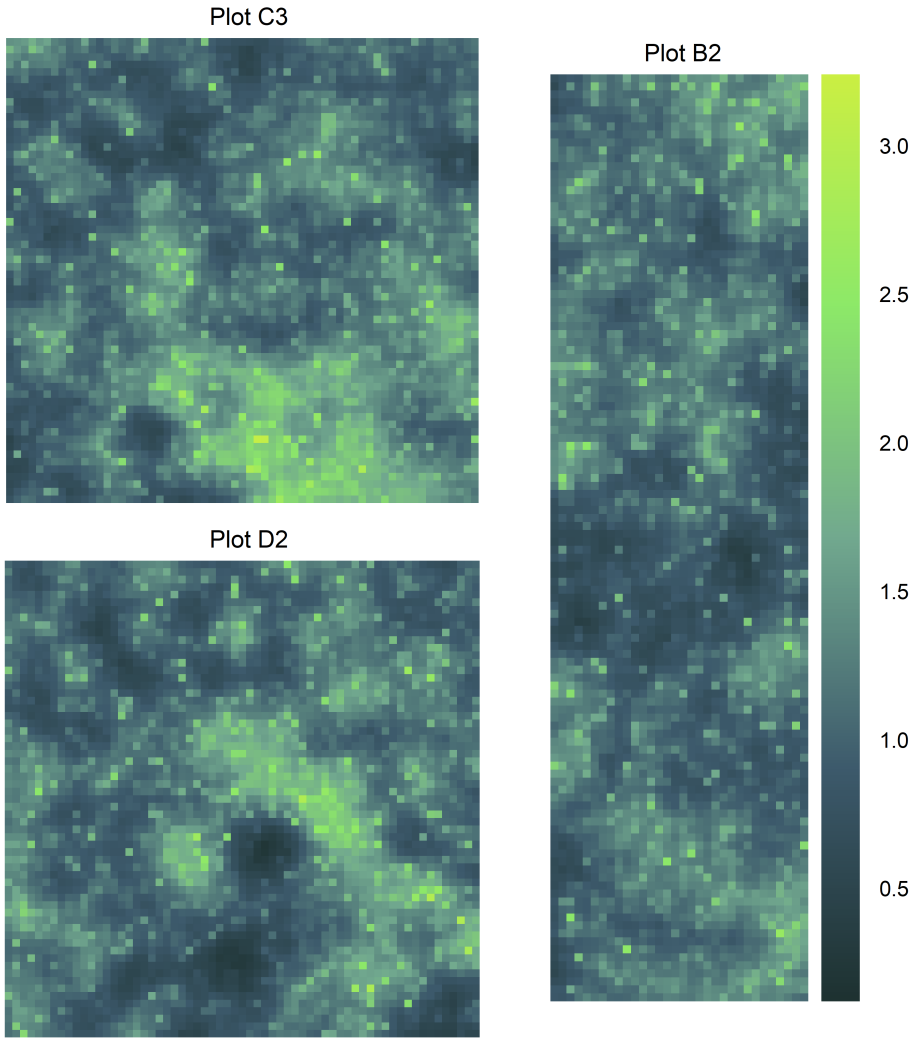

Figure C.2: Plot neighborhood density index (radians).

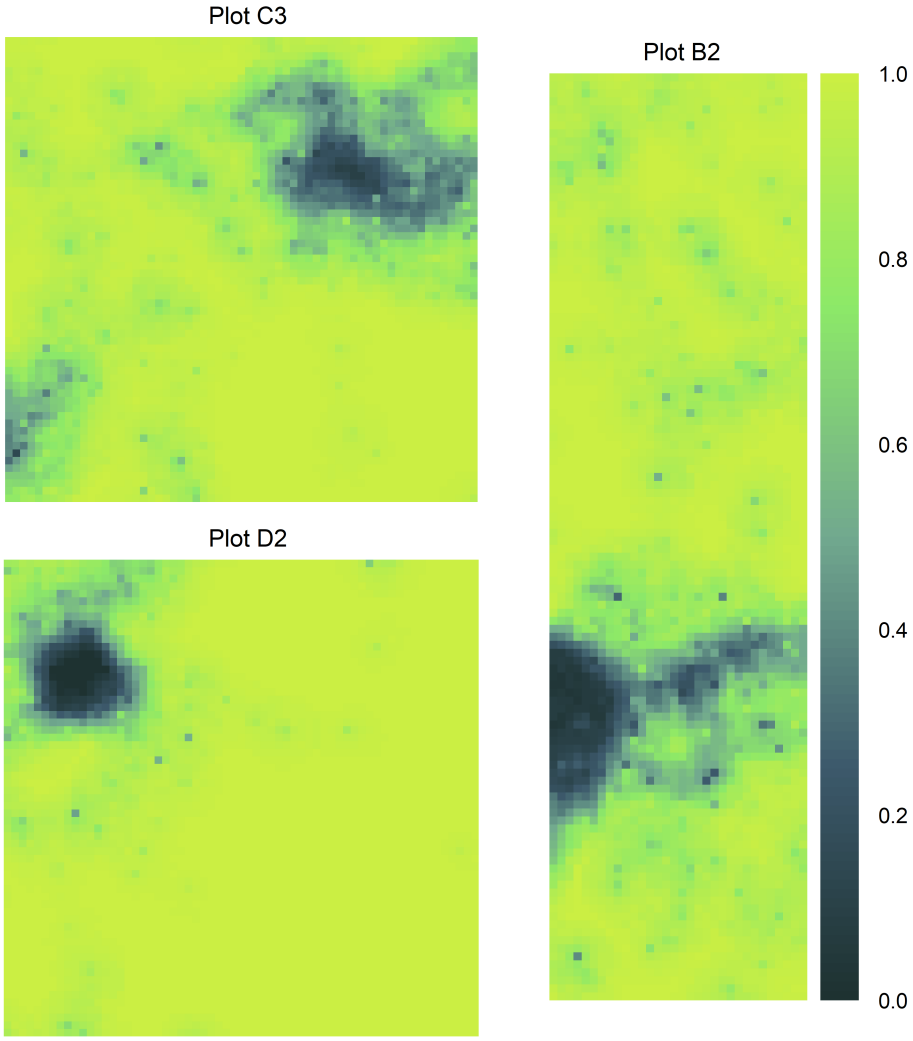

Figure C.3: Plot neighborhood host proportion.

Appendix D

TRIANGULATION OF THE STUDY REGION

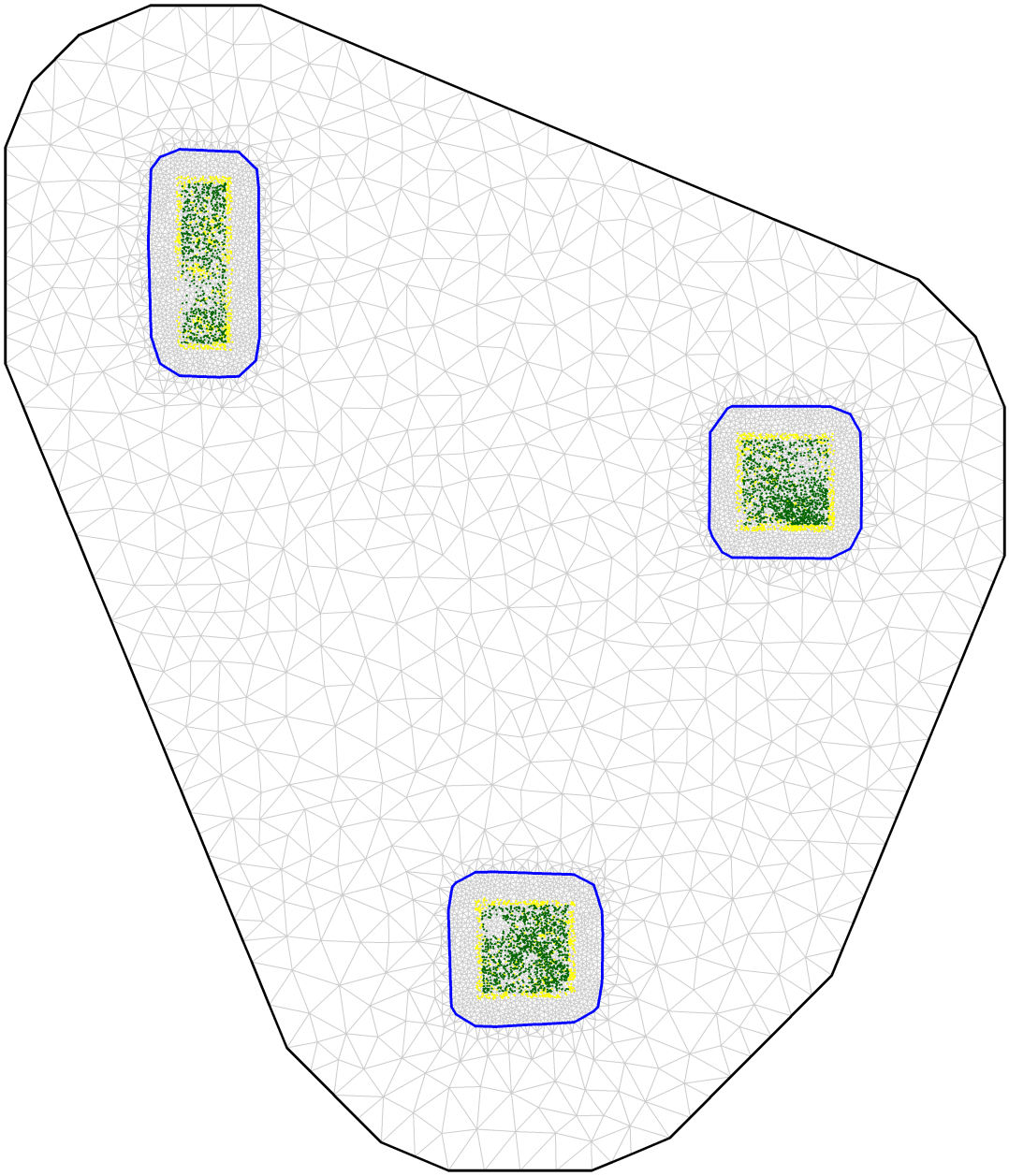

Figure D.1: Triangulation of the study region, used in the SPDE approach. Yellow dots represent all lodgepole pine alive and ≥5 cm DBH in 2004. Green dots represent lodgepole pine used in modeling (i.e., those >10 m from the edge of the plot and with growth data preceding the outbreak).

Appendix E

MODEL SUMMARY

	Mean	SD	0.025quant	Median	0.975quant
Fixed effects:					
Intercept	0.567	0.093	0.387	0.566	0.753
DBH	5.608	0.232	5.162	5.604	6.074
BAI	0.269	0.151	-0.025	0.268	0.567
NDI	0.869	0.171	0.537	0.868	1.209
pNDI	0.241	0.140	-0.032	0.241	0.517
TPI	0.098	0.130	-0.159	0.099	0.352
DBH:BAI	-0.777	0.376	-1.478	-0.790	0.000
DBH:NDI	0.969	0.392	0.204	0.967	1.743
DBH:pNDI	0.891	0.261	0.354	0.899	1.380
DBH:TPI	0.310	0.324	-0.330	0.311	0.943
PlotC3	0.102	0.251	-0.385	0.098	0.606
PlotD2	1.182	0.255	0.678	1.182	1.684
Model hyperparameters for random effects:					
Range for s	33.264	9.726	18.827	31.67	56.664
Stdev for s	0.512	0.097	0.341	0.506	0.721

Table E.1: Summary of model fixed effects and hyperparameters.

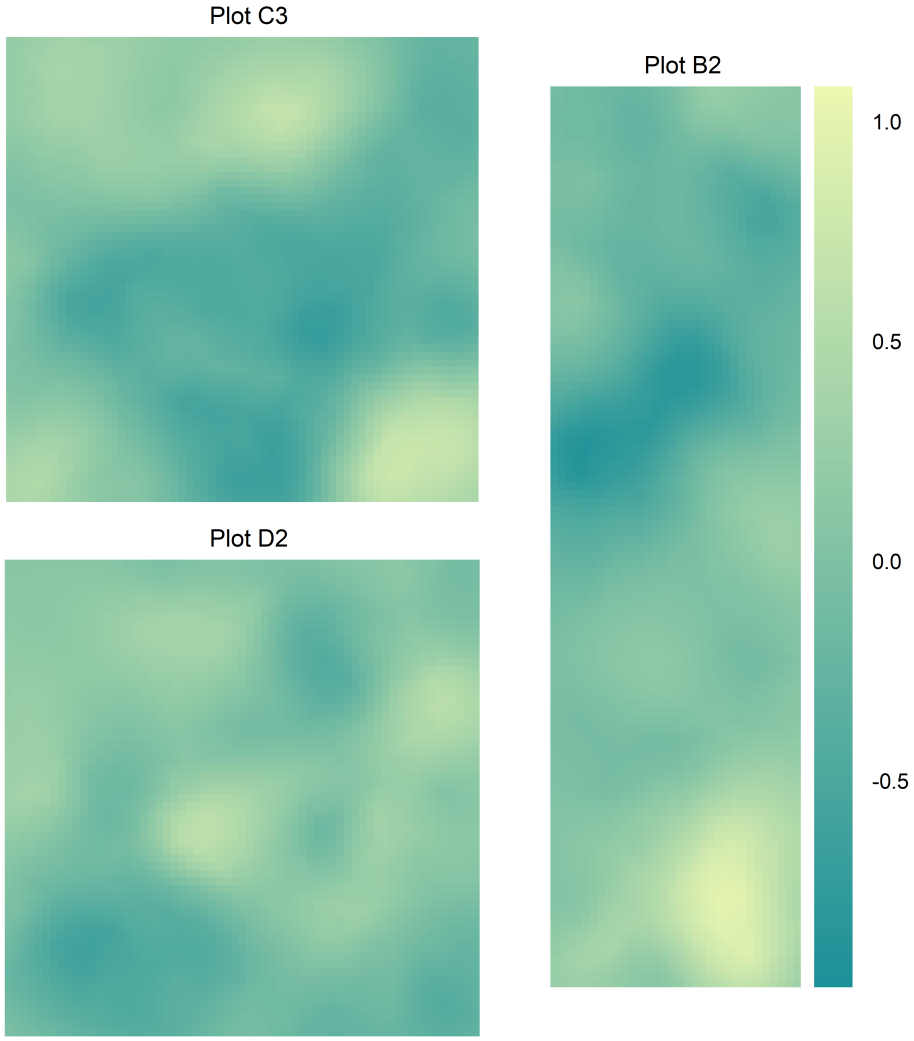

Figure E.1: Posterior mean of the spatial Gaussian random field, which is added to the linear predictor in logit space.

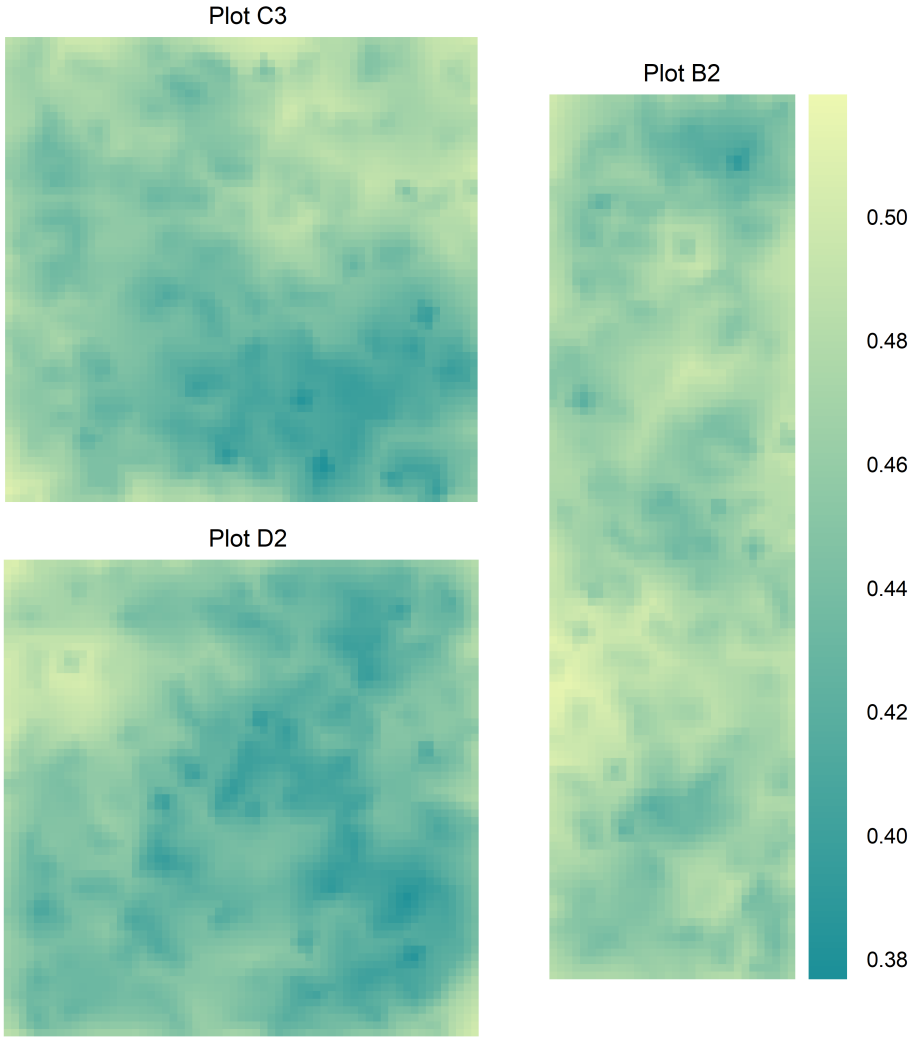

Figure E.2: Posterior standard deviation of the spatial Gaussian random field, which is added to the linear predictor in logit space.

Appendix F

COMPARISON OF SPATIAL AND NON-SPATIAL MODEL PREDICTIONS

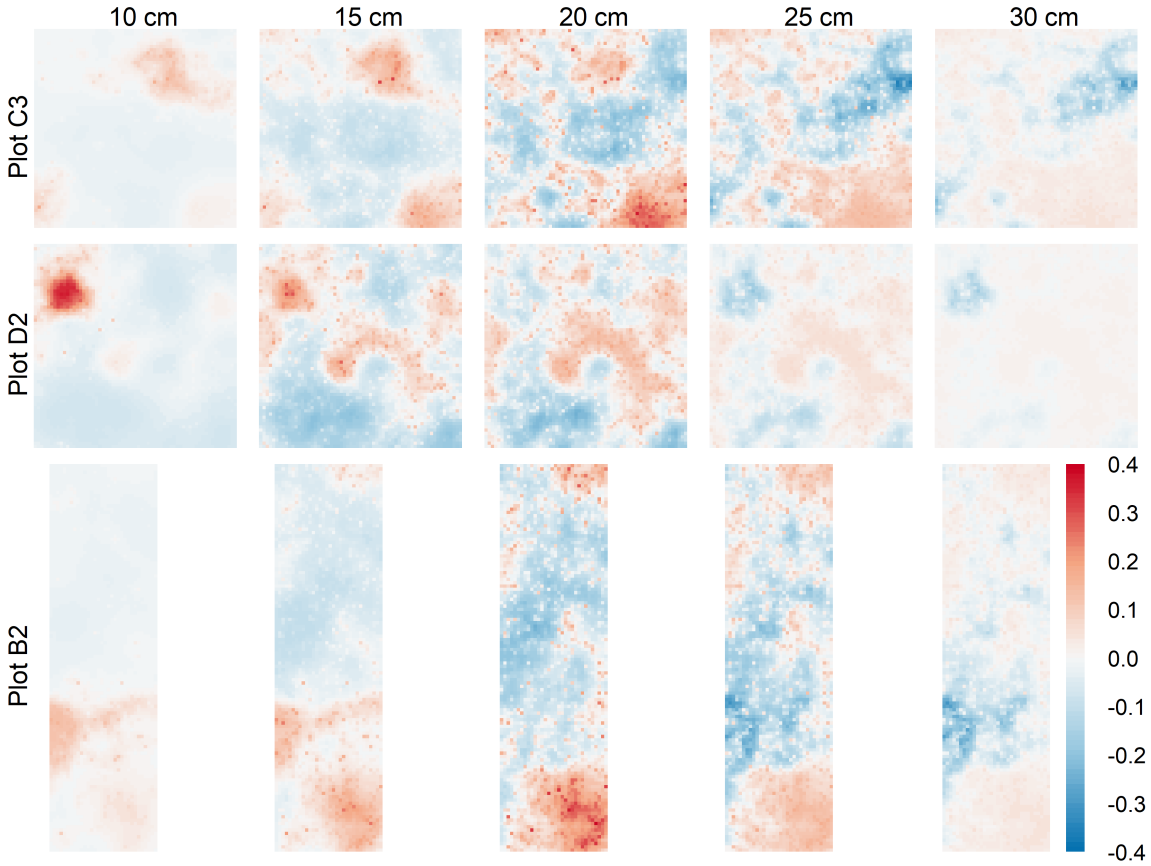

Figure F.1: Difference in posterior median predicted mortality probability for a range of lodgepole pine DBH (10 to 30 cm) when adding the spatial GRF and neighborhood level covariates to a model that includes only plot and tree level covariates. Predicted mortality probability is based on the specified DBH (columns) and the values of NDI, pNDI, and the spatial GRF for a hypothetical tree located within each grid cell in each plot (rows). BAI and TPI were held at zero (i.e., their average values).

Appendix G

SENSITIVITY ANALYSIS

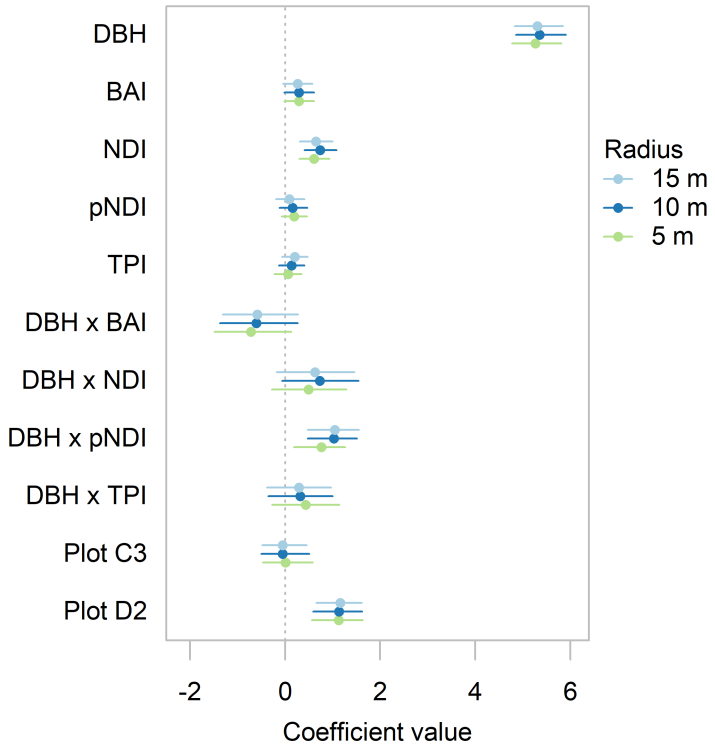

Figure G.1: Effect of neighborhood radius on model coefficients. Dots represent the medians of the posteriors and horizontal lines represent 95% credible intervals. The effects for each continuous predictor are per 2 standard deviations in logit space. To enable comparison, trees <15 from the edge of each plot were excluded from each of the models.